

Utility of Light Emitting Diodes for Inter-satellite Communication in Multi-Satellite Networks

David N. Amanor
ECE Department
North Carolina A&T State University
Greensboro, NC 27401
Email: dnamanor@aggies.ncat.edu

William W. Edmonson
ECE Department
North Carolina A&T State University
Greensboro, NC 27401
Email: wwwedmons@ncat.edu

Fatemeh Afghah
EECS Department
Northern Arizona University
Flagstaff, Arizona 86001
Email: fatemeh.afghah@nau.edu

Abstract—Future space missions will be designed to take advantage of multi-satellite network deployment because of their potential for providing improved spatial and temporal resolutions of a target and/or can provide a more comprehensive observation of the Earth. To enable interoperability within this satellite network particularly for autonomous operations and provide on-orbit data handling through distributed processing, a reliable inter-satellite communication (ISC) is required. In this paper, we examine the suitability of Light-Emitting Diodes (LEDs) for ISC in multi-satellite networks, and further propose an approach of the physical layer design that meets the requirements of the platform in terms of the size, weight and power (SWaP) of the satellite. An analytical model of the ISL is developed to test feasibility of using LEDs for reliable data communication in the presence of steady solar background illumination. Finally, the performance of the ISL is evaluated in terms of the Bit Error Rate (BER) and achievable data rates for four different intensity modulation and direct detection (IM/DD) schemes.

I. INTRODUCTION

The shift from using large and expensive satellites to multiple low-cost small satellites deployed as a sensor network for space exploration has necessitated the need for inter-satellite communication (ISC). Presently, the dominant research and development for implementing inter-satellite communication links (ISLs) consists of using either radio frequency (RF) or highly directed lasers. The latter will require a highly accurate pointing satellite control system and limited available spectrum to support high data rates, while the former is not suitable for systems with sensitive electronics onboard. The required pointing precision needed for laser communication may not be possible for small satellites due to the stringent SWaP constraints imposed by the platform. Furthermore, for multi-satellite networks in low earth orbit (LEO), the ISLs are much shorter in length than links between satellites in geostationary orbit; thus, the use of lasers and the extremely accurate pointing they offer can be considered superfluous for such applications [1]. To reduce the SWaP constraints imposed by the platform, along with the need for reduced pointing accuracy and to achieve high data transmission rates, we propose a visible light communication (VLC) subsystem for pico-/nanoclass of satellites for ISC.

In this paper, we examine the feasibility of using LEDs for ISC in multi-satellite networks in the presence of steady background illumination through a novel design of the physical layer. We developed an analytical model of the complete VLC

link including solar background radiation to test feasibility of the proposed system, and further evaluated the performance of the link for four different intensity modulation and direct detection (IM/DD) schemes.

The main contribution of this paper is, to the best of our knowledge, the first work that covers quantitative assessment of solar background illumination and its impact on ISC using visible light for small satellites. Additionally, the use of natural low-background noise channels (i.e., Fraunhofer lines) for VLC systems of medium scope using LEDs is a concept which has been investigated in this work.

The rest of the paper is organized as follows. After a brief review of related works in Section II, the proposed system description was presented in Section III. These include the key design considerations, VLC link physical model, transmitter, and channel models as well as solar background noise model. In Section IV, we performed numerical analysis and evaluated the link performance through a Matlab implementation of the analytical model for On-Off Keying (OOK-NRZ), L-Level Pulse Position Modulation (L-PPM), Asymmetrically Clipped Optical OFDM (ACO-OFDM) and DC-biased Optical OFDM (DCO-OFDM). The conclusion of the paper is captured in Section V.

II. RELATED WORKS

The concept of using light as a communication medium predates the transmission of speech by radio, but the difficulty in transmitting light beam from point to point due to obstacles along the path discouraged further research at the time [2]. However, recent advancement in LED technology has triggered renewed interest in VLC as a viable alternative to RF and laser for line-of-sight (LOS) communication links of moderate scope.

In [1], the utility of LEDs for short-range ISLs were examined for a hypothetical low-end LED ISL. The work discussed methods for minimizing background illumination, but did not examine, in quantitative terms, the impact of solar background on link performance. In [3], LEDs were evaluated and flown in orbit for intra-satellite communication between internal assemblies onboard satellites, but were not used for ISC. These lamps combine very low-power consumption with an extremely long operational life, maintaining during all their operation the same chromaticity without significant

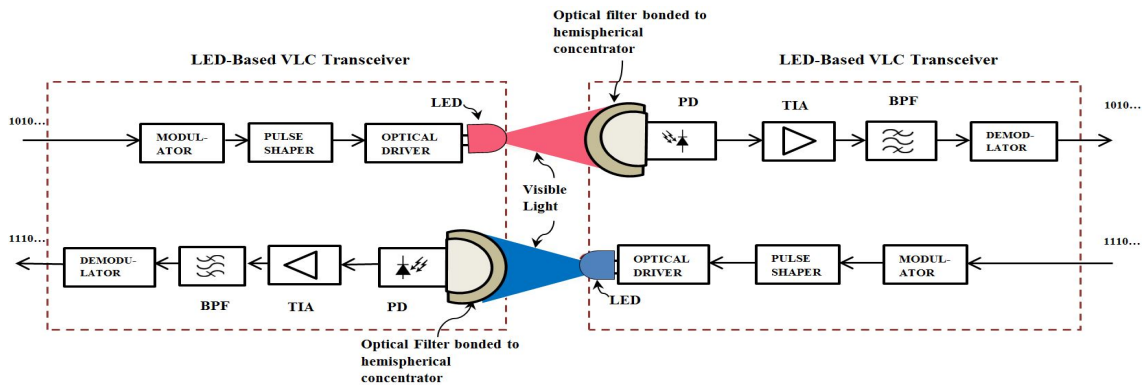


Fig. 1: Conceptual Architecture of Full Duplex VLC System for ISC for Small Satellites

changes. Komine [4] discusses the fundamental analysis for VLC system using LED lights for indoor applications.

Similarly, research in using VLC for short-range data communications particularly for the automotive industry and smart lighting applications is attracting significant attention [5],[6].

For outdoor VLC systems using LEDs, the main limitation to reliable data communications is the intense solar background power, which is usually greater than the intensity-modulated information signal. Based on our review of literature, we have not sighted any paper that covered quantitative assessment of solar background illumination and its impact on ISC for small satellites.

III. PROPOSED SYSTEM DESCRIPTION

A block diagram of the proposed full duplex VLC system architecture is shown in Fig. 1. In this paper we will focus on the development of the VLC physical layer as represented by OSI.

The conceptual underpinning for the physical layer design is the use of dark absorption lines in the Sun's output (i.e., Fraunhofer lines) as natural low background noise channels for signal transmission. A photodetector (PD) placed behind a filter tuned to a specific Fraunhofer line will not be perturbed with the Sun's interference [1]. This leads to the establishment of a natural low background noise link between any two small satellites in LOS configuration using LED(s) at the transmitter and PD(s) at the receiver.

The design of the receiver's optical front-end follows the approach proposed in [7] in order to take advantage of the high gain of the hemispherical lense and a narrow-band, wide FOV optical front-end. It was shown in [7] that the gain of the hemispherical front-end is nearly omni-directional which makes it a more useful configuration to deploy in a wide FOV application; under certain conditions, the optical gain of a hemispherical concentrator of index n is approximately n^2 , regardless of the angle of incidence. The hemispherical front-end is also more robust to receiver movements and FOV misalignments compared to a planar optical front-end.

We used PIN photodiode because the background light is generally large enough that the resulting shot noise dominates the thermal noise produced within the electrical front-end. This

is preceded by a narrowband optical filter which is tuned to the selected Fraunhofer line.

A. Design Considerations

In this subsection, we review the key design considerations for the proposed system.

1) *Approach to Mitigate Background Noise:* The radiative energy per cross-sectional unit area that the Sun emits to the Earth system across all wavelengths of the electromagnetic spectrum based on Planck's radiation formula is $1360W/m^2$. The equivalent radiative energy within the visible light spectrum only (i.e., 380 nm to 750 nm) is approximately $595W/m^2$. This intense background power poses the single biggest challenge to free space optical communications.

In this work, we propose to place a PIN photodiode behind a narrowband optical filter, which is tuned to a Fraunhofer line in order to avoid any perturbation from the Sun's interference.

At the most intense Fraunhofer lines, the solar background falls below 10 percent of its continuum values [8].

2) *Doppler Effect:* A fundamental problem that needs to be addressed for ISC between two satellites is Doppler effects. A Doppler shift causes the received signal frequency of a source to differ from the sent frequency due to motion that is increasing or decreasing the distance between the source and receiver. The impact of Doppler effects on the performance of inter-satellite links has been studied in [9]. The normalized wavelength shift between a transmitting and receiving satellite is given by [9]:

$$\Delta\lambda = \frac{\lambda_s}{c} \frac{d}{dt} |r(t, \tau)| \quad (1)$$

where $\Delta\lambda = \lambda_d - \lambda_s$ and $\Delta\lambda$ stands for normalized Doppler wavelength shift; λ_d and λ_s are the wavelengths of the received signal and emitted signal respectively. $r(t, \tau)$ represents the actual propagation range of the signal from the source satellite to destination.

It follows from (1) that no Doppler shift can be detected when the distance between the source and destination satellites is maintained constant. In this work, we focus on ISC for satellites within the same orbital plane where the effect of Doppler shifts is assumed to be negligible.

3) *Spectrum Band for Transmission*: We propose frequency bands with LED peak wavelength centered on Fraunhofer lines. Table I is a list of deep Fraunhofer lines that can be used for our proposed application. The peak wavelength is a function of the LED chip material and is the wavelength at which the LED emits peak power; this wavelength must be matched to the wavelengths that are transmitted with the least attenuation through the channel. Fraunhofer lines with bandwidth greater than 250 GHz were chosen in order to ensure that any Doppler shifts that may cause marginal shifts of the targeted Fraunhofer line can be accommodated.

TABLE I: Proposed Fraunhofer Lines for ISC using Visible Light

LED Peak Wavelength (nm)	Bandwidth (nm)	Bandwidth (GHz)
381.5851	0.1272	262.1
382.0436	0.1712	351.9
382.5891	0.1519	311.3
383.2310	0.1685	344.2
383.8302	0.1920	391.0
385.9922	0.1554	312.9
393.3682	2.0253	3926.6
396.8492	1.5467	2946.3
410.1748	0.3133	558.7
434.0475	0.2855	454.6
486.1342	0.3680	467.2
656.2808	0.4020	280.0

4) *Bandwidth and Data-rate*: The visible light band has enormous potential for data communication with very high data rates. However, unlike RF communication, the data rate of VLC is limited by the switching speed of the LED transmitter. The switching speed is measured as the LEDs rise and fall time that is required to go from 10 percent to 90 percent of peak power. The LED must switch fast enough to meet the bandwidth requirements of the system.

5) *LED Specification*: The most important types of LEDs that can be used for VLC have been summarized in [10]. These are Phosphor Converted LEDs (pc-LEDs), Multi-chip LEDs, Micro LEDs (-LEDs) and Resonance Cavity LEDs (rc-LEDs). The pc-LEDs are low cost but have a bandwidth limitation which restricts the direct modulation frequency to a few MHz due to the slow response of the phosphor. Multi-chip LEDs uses three or more LED chips which emit different colors to produce white light. They have the merit of producing three different color channels to support multiple or parallel transmissions each with a bandwidth of about 15 MHz. Micro-LEDs are currently being developed and have the potential to support high density parallel communication allowing speeds of up to 1.5 Gbps. Resonance Cavity LEDs are particularly suited for optical data communication via Plastic Optical Fiber (POF) and IR wireless communication.

In addition to their capability in supporting multiple transmissions, multi-colored LEDs also brings the needed adaptability for the implementation of the front-end as Software Defined Optics (SDO).

6) *Photodetectors*: Several factors influence the choice of a detector for a given application. Key among these include the light power level, wavelength range of the incident light,

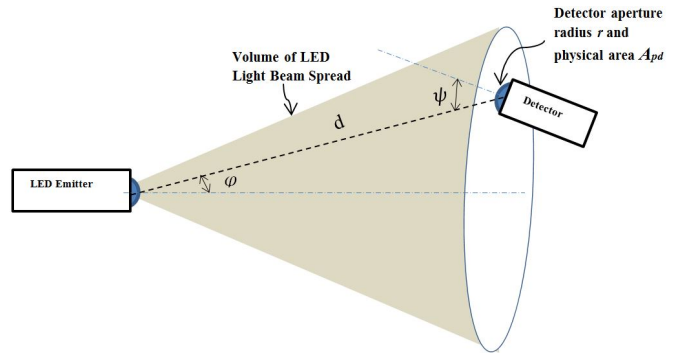


Fig. 2: LOS VLC Link Model: Adapted from [11]

electrical bandwidth of the detector amplifier and the mechanical requirements of the application, such as size or temperature range of operation. Also important are cost, and the environment which includes the platform. Most often, these criteria will limit the options for a given application.

PIN photodiodes and avalanche photodiodes (APD) have been widely used in many experimental studies on free space optical communication including VLC [1]-[7]. APDs are advantageous over PIN photodiodes in applications where the dominant noise is the electrical noise in the pre-amplifier, rather than shot noise. However, in wireless systems, the background light is generally large enough that the resulting shot noise overshadows the thermal noise produced within the amplifiers and load resistors internal to the detection system, thus limiting the usefulness of APDs for outdoor optical wireless communication systems.

B. VLC Link Physical Model

We can model the general LOS link between any two adjacent satellites in a trailing (or leader-follower) formation or within a cluster according to the LOS VLC scenario set out in Fig. 2.

The receiver's front-end is depicted as in Fig.1 and consists of a narrowband optical filter bonded to a hemispherical concentrator while an LED emitter is the main constituent at transmitter front-end. The distance of the receiver from the LED emitter is denoted by d , while the receiver aperture radius and detector physical area are represented by r and A_{pd} , respectively. The angle of incidence with respect to the receiver axis is ψ and the angle of irradiance with respect to the transmitter perpendicular axis is φ . Angle φ is sometimes referred to as viewing angle as it indicates how focused the beam is when emitted from the LED.

For a given receiver FOV, the effective signal-collection area A_{eff} of the detector is given by $A_{eff} = A_{pd} \cos \psi$ where $\psi < FOV$.

C. Transmitter Model

We modelled the LED transmitter as a generalized Lambertian radiation source of order m , where the radiant power $R(\varphi)$ in Watts per steradian (W/Sr) at an angle φ is given by [11]

$$R(\varphi) = \frac{(m+1)}{2\pi} P_t (\cos\varphi)^m \quad (2)$$

where φ is in the range $\frac{\pi}{2}$ to $\frac{-\pi}{2}$, m is a number describing the directivity of the radiation pattern and $m > 0$. P_t is the total power radiated by the LED and φ is the angle of irradiance with respect to the LED transmitter perpendicular axis. For generalized Lambertian radiation pattern, the optical signal becomes more directional as m increases.

D. Channel Model

The VLC channel between two small satellites can be modeled as an Additive White Gaussian Noise (AWGN) channel with four key parameters, namely, the photodiode current $Y(t)$, input optical power $X(t)$, channel impulse response $h(t)$ and the Gaussian noise $N(t)$ [7],[13];

$$Y(t) = \gamma X(t) \otimes h(t) + N(t) \quad (3)$$

where γ represents the responsivity of the photodetector (in A/W) and \otimes denotes linear convolution.

For LOS optical links, the single most important quantity for characterizing the channel is the DC Gain, $H(0)$ [7],[13], which relates the received optical power P_r to the transmitted optical power P_t as shown in (4)

$$P_r = H(0)P_t \quad (4)$$

The channel DC Gain is given by $H(0) = \int_{-\infty}^{\infty} h(t)dt$ [12], where $h(t)$ represents the impulse response of the channel.

Following the analysis in [12], the channel gain in LOS links can be estimated fairly accurately by considering only the LOS propagation path and can be expressed as

$$H(0) = \begin{cases} \frac{(m+1)}{2\pi d^2} A_{pd} (\cos\varphi)^m T_s(\psi) g(\psi) \cos(\psi), & : 0 \leq \psi \leq \psi_c \\ 0, & : \psi > \psi_c \end{cases} \quad (5)$$

where $T_s(\psi)$ and $g(\psi)$ represents the filter transmission coefficient (or gain) and concentrator gain, respectively. ψ_c is the concentrator FOV semi-angle and m is a number describing the shape of the radiation characteristics (i.e., the order of Lambertian emission). The Lambertian order m is related to the semi-angle at half illuminance of an LED, $\phi_{\frac{1}{2}}$ and is given by [11].

$$m = \frac{-\ln 2}{\ln(\cos(\phi_{\frac{1}{2}}))} \quad (6)$$

By using a hemispherical lens (i.e., non-imaging concentrator) with internal refractive index n , we can achieve a gain of [7]

$$g(\psi) = \begin{cases} \frac{n^2}{\sin^2\psi_c} & : 0 \leq \psi \leq \psi_c \\ 0, & : \psi > \psi_c \end{cases} \quad (7)$$

A hemisphere can achieve $\psi_c \approx \frac{\pi}{2}$ and $g(\psi) \approx n^2$ over its entire FOV provided the hemisphere is sufficiently large

in relation to the detector, i.e., $R > n^2 r$, where r and R represents the detector and hemisphere radii, respectively [12].

The electrical signal component at the receiver side is given by [13]

$$S = (\gamma P_r)^2 \quad (8)$$

E. Solar Background Model

Background radiation from extended sources such as stars and reflected background radiation are assumed to be too weak to be considered for terrestrial Free Space Optical (FSO) links; however, they contribute significantly to background noise in deep space FSO. In this work, we consider the Sun as the main source of background radiation in our proposed system. We modelled the Sun as a blackbody using Planck's blackbody radiation model, in which Spectral irradiance of the source is a function of wavelength and temperature [13], i.e.,

$$W(\lambda, T) = \frac{2\pi h_p c^2}{\lambda^5} \frac{1}{(e^{\frac{h_p c}{\lambda k T}} - 1)} \quad (9)$$

where λ is the wavelength, c is the speed of light, h_p is Planck's constant, k is Boltzmann's constant and T is average temperature of the Sun's surface.

Following the work of Spencer, [14], we developed a simple yet fairly accurate analytical model that describes the irradiance that falls within the spectral range of the receiver optical filter as in (10)

$$E_{det} \approx 2.15039 \times 10^{-5} d_f t_f \int_{\lambda_a}^{\lambda_b} W(\lambda, T) d\lambda \quad (10)$$

where d_f and t_f are coefficients that represents the *day of the year* and *time of day*, respectively and can be computed as in [14]. In this paper, we assumed the worst case scenario, i.e., around midday when there is peak irradiance and the Sun is directly overhead the optical front-end of the receiver; thus, solar zenith angle is zero and t_f is 1.0. The constant, 2.15039×10^{-5} is the ratio of the surface area of the Sun to the surface area of the sphere with radius centered at the Sun and length of one astronomical unit.

We validated our model by evaluating (10) for different wavelength intervals and compared the results with Solar Fluxes (W/m^2) taken from the 1985 Wehrli Standard Extraterrestrial Solar Irradiance Spectrum [15].

Therefore, the background noise power detected by the optical receiver physical area is given by [7]:

$$P_{bg} = E_{det} T_o A_{pd} n^2 \quad (11)$$

where T_o is the filter transmission coefficient and n is the internal refractive index of the concentrator at the receivers optical front end.

The total input noise variance N is the sum of the variances of the shot noise and thermal noise [7]:

$$N = \sigma_{shot}^2 + \sigma_{thermal}^2 \quad (12)$$

We neglect the effects of intersymbol interference (ISI) based on the assumption that the inter-satellite link between

any two adjacent satellites in a leader-follower or cluster formation is not amenable to multipath propagation.

The shot noise variance is given by [13]

$$\sigma_{shot}^2 = 2q\gamma(P_r + I_2P_{bg})B \quad (13)$$

where q is the electronic charge, B is the equivalent noise bandwidth, γ represents the photodetector responsivity, and I_2 is the noise bandwidth factor for a rectangular transmitter pulse.

Following the analysis in [7], the thermal noise variance can be expressed by:

$$\sigma_{thermal}^2 = \frac{8\pi kT_A}{G}\eta A_{pd}I_2B^2 + \frac{16\pi^2 kT_A\Gamma}{g_m}\eta^2 A_{pd}^2 I_3 B^3 \quad (14)$$

where k is Boltzmanns constant, T_A is the absolute temperature, G is the open-loop voltage gain, η is the fixed capacitance of photodetector per unit area, Γ is the FET channel noise factor, g_m is the FET transconductance and I_3 is the noise bandwidth factor for a full raised-cosine pulse shape [7].

Finally, the electrical SNR at the receiver, which is a key metric for measuring the quality of the communication link, can be determined by

$$SNR = \frac{S}{N} = \frac{(\gamma P_r)^2}{\sigma_{shot}^2 + \sigma_{thermal}^2} \quad (15)$$

F. Modulation Scheme

A key difference between VLC and RF communication is in the way data is encoded. While data can be encoded in the amplitude or phase of an RF signal, signal intensity is the primary parameter used for conveying information in VLC systems. The implication is that phase and amplitude modulation techniques cannot be applied in VLC; rather the data has to be encoded in the varying intensity of the emitting light pulses. At the receiver side, direct detection is the dominant approach for signal recovery due to changes in the instantaneous power of the transmitted signal. Thus, intensity modulation and direct detection (IM/DD) schemes are the main modulation/demodulation methods used in VLC systems. A further attribute of an IM/DD system is that the modulating signal must be both real valued and unipolar. This distinctive feature of VLC, as an IM/DD system, has profound consequence on the type of modulation scheme to use.

A detailed review and comparison of different modulation schemes was carried out in [16]. In this paper, we will investigate the performance of the proposed VLC link for OOK-NRZ, L-PPM modulation, ACO-OFDM and DCO-OFDM. Table III is a summary of methods for determining the BER and achievable data rate for four different modulation schemes.

IV. NUMERICAL ANALYSIS AND RESULTS

We used the numerical values in Table III for the simulation of our analytical model and set the parameter t_f in (10) to 1.0 (i.e., peak irradiance) in order to evaluate the performance of the link for the worst case background noise scenario. The

TABLE II: Methods for BER and Achievable Data Rates [16]

Modulation Scheme	BER	Achievable Data Rate (bits/s)
OOK-NRZ	$\frac{1}{2} \operatorname{erfc}(\frac{1}{2\sqrt{2}}\sqrt{SNR})$	B
L-PPM	$\frac{1}{2} \operatorname{erfc}(\frac{1}{2\sqrt{2}}\sqrt{SNR\frac{L}{2}\log_2 L})$	$B\frac{\log_2 L}{L}$
DCO-OFDM	$\frac{\sqrt{M}-1}{\sqrt{M\log_2 L\sqrt{M}}}\operatorname{erfc}(\sqrt{\frac{3SNR}{2(M-1)}})$	$\frac{\frac{N}{2}-1}{N+N_g}(B\log_2 M)$
ACO-OFDM	$\frac{\sqrt{M}-1}{\sqrt{M\log_2 L\sqrt{M}}}\operatorname{erfc}(\sqrt{\frac{3SNR}{2(M-1)}})$	$\frac{\frac{N}{4}-1}{N+N_g}(B\log_2 M)$

optical filter at the receiver front-end is tuned to the deep Fraunhofer line at 656.2808 nm wavelength with a line width of 0.4020 nm. Based on the setting of the optical filter, we assumed that the solar background admitted by the optical filter is less than 10 percent of its continuum values [8]. The continuum value of the background noise power detected by the optical receiver physical area can be computed based on eqns. (10) and (11). We used a 28 mm x 28 mm Si PIN Photodiode (S3584) from Hamamatsu with its corresponding responsivity [17].

TABLE III: Simulation Model Parameter Assumptions

Parameter	Value
Transmitted Optical Power, P_t	2 W
Semi-angle at Half Power, $\Phi_{\frac{1}{2}}$	30°
LED Peak Wavelength, λ_{peak}	656.2808 nm
Concentrator FoV Semi-angle, ψ_c	Varied: 35°, 45° & 60°
Filter Transmission Coefficient, T_o	1.0
Incidence Angle, φ	30°
Irradiance Angle, ψ	15°
Detector Responsivity, γ	0.51
Refractive Index of Lens, n	1.5
Radius of Concentrator, R	2.0 cm
Detector Active Area, A_{pd}	2.8 cm x 2.8 cm
Assumed Electrical Bandwidth, B	0.5 MHz
Optical Filter Bandwidth, $\Delta\lambda$	0.4020 nm
Optical Filter Lower Limit, λ_1	656.0798 nm
Optical Filter Upper Limit, λ_2	656.4818 nm
Open Loop Voltage Gain, G	10
FET Transconductance, g_m	30 ms
FET Channel Noise Factor, Γ	0.82
Capacitance of Photodetector, η	38 pF/cm ²
Link Distance, d	Varied: 1 km - 3 km
Background Noise Power, P_{bg}	1 mW
Noise Bandwidth Factor for White Noise, I_2	0.562
Noise Bandwidth Factor for f^2 noise, I_3	0.0868
Boltzmann Constant, k	1.3806488x10 ⁻²³ J/K
Absolute Temperature, T_A	300 K

Fig. 3 is a plot of the SNR for different values of concentrator FoV. Clearly, the impact of the concentrator FoV on the SNR is apparent. A 10° reduction in the FoV semi-angle translates into an improvement of the SNR by about 3.5 dB. However, because we desire a narrow-band, wide FoV optical front-end, we are constrained by the extent to which we can reduce the concentrator FoV. It is important, following the analysis in [7], that the concentrator FoV semi-angle, ψ_c is greater than the incidence angle, φ in order to achieve a concentrator gain $g(\psi)$ of n^2 or greater.

The BER performance of the link under different background noise conditions and concentrator FoVs is captured

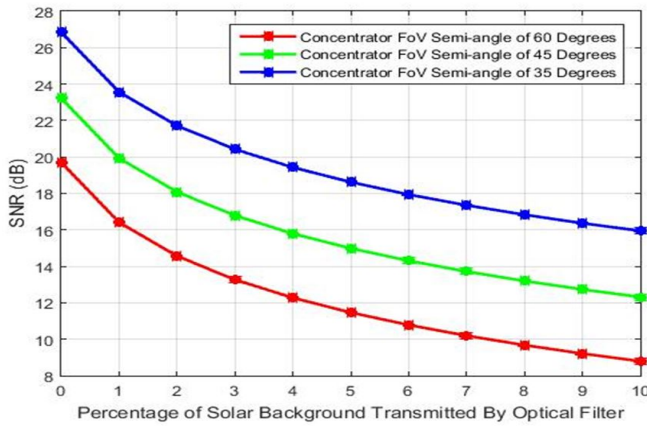


Fig. 3: Impact of Solar Background on SNR for Link Distance of 0.5 km, Transmitted Optical Power Output of 2W and assumed Electrical Bandwidth of 0.5 MHz

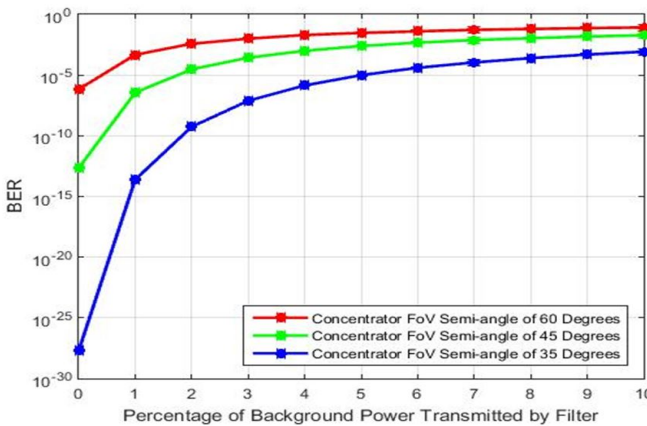


Fig. 4: BER Plot for Link Distance of 0.5 km, Transmitted Optical Power Output of 2W, and Electrical Bandwidth of 0.5 MHz for Different Concentrator FoV

in Fig. 4. We assumed OOK-NRZ modulation where the achievable data rate is equal to the bandwidth. We achieved a data rate of 0.5 Mbits/s for a link distance of 0.5 km at a BER of 10^{-6} for a concentrator FoV semi-angle of 35° . A BER of 10^{-6} is the performance requirement for stable communication link [13]. L-PPM modulation for $L > 2$ achieves a better BER performance than OOK-NRZ as shown in Table IV, but at the detriment of significant decrease in data-rate. By moving to higher-order constellation, M , it is possible to achieve a higher data-rate with ACO-OFDM and DCO-OFDM compared to OOK-NRZ based on Table II. However, for the same SNR, the BER of OOK-NRZ and L-PPM performs better than ACO-OFDM and DCO-OFDM as the constellation order increases.

V. CONCLUSION

The main limitation of outdoor VLC systems using LEDs is the relatively high solar background irradiance, which degrades the SNR at the receiver. Thus, the physical layer design must deliberately include mitigating techniques to minimize

TABLE IV: BER Analysis of Different Modulation Schemes

Modulation Scheme	BER
OOK-NRZ	9.9×10^{-6}
L-PPM	$L = 2$; 9.9×10^{-6}
	$L = 4$; 7.2×10^{-18}
	$L = 8$; 7.2×10^{-49}
DCO-OFDM	$M = 2$; 1.2×10^{-49}
	$M = 4$; 7.2×10^{-18}
	$M = 8$; 1.0×10^{-8}
ACO-OFDM	$M = 2$; 1.2×10^{-49}
	$M = 4$; 7.2×10^{-18}
	$M = 8$; 1.0×10^{-8}

the impact of background power without violating the SWaP constraints of the small satellites platform.

In this paper, we demonstrated the feasibility of establishing reliable inter-satellite links for small satellites in the presence of steady background illumination using natural low-background noise channels, LEDs and PIN photodiode. Using OOK-NRZ modulation scheme, we achieved a data rate of 0.5 Mbits/s for a moderate link distance of 0.5 km at a BER of 10^{-6} , which is the performance requirement for stable communication link. The above data rate is sufficient to support navigation, command and health data as well as some portion of science data.

REFERENCES

- [1] L. Wood and W. Dorpelkus, *Using Light-Emitting Diodes for Intersatellite Links*, IEEE Aerospace Conference, 2010
- [2] R. Sagotra and R. Aggarwal, *Visible Light Communication*, International Journal of Engineering Trends and Technology, Vol. 4, Issue 3, 2013
- [3] I. Arruego, et al., *OWLS: A Ten-Year History in Optical Wireless Links for intra-Satellite Communications*, IEEE Journal on Selected Areas in Communications, to appear, first quarter 2010
- [4] T. Komine, *Fundamental Analysis for Visible-Light Communication System using LED Lights*, IEEE Transactions on Consumer Electronics, Vol. 50, Issue 1, Feb. 2004
- [5] C. Liu, et al., *Enabling vehicular visible light communication (V2LC) networks*, Proceedings of the Eighth ACM international workshop on Vehicular inter-networking, ser. VANET, New York, 2011
- [6] A. Cailean, et al., *Visible light communications: Application to cooperation between vehicles and road infrastructures*, IEEE Intelligent Vehicles Symposium (IV), 2012, pp. 10551059.
- [7] J. Barry, *Wireless Infrared Communications*, Kluwer Academic Publishers, ISBN 0-7923-9476-3
- [8] J. Gelbwachs and M. Tabat, *Solar Background Rejection by Pressure Broadened Atomic Resonance Filter Operating at a Fraunhofer Wavelength*, Optics Letters, Vol.
- [9] Q. Yang, et al., *Doppler characterization of laser inter-satellite links for optical LEO satellite constellations*, Optics Communications, 2009
- [10] C. Medina, et al., *LED Based Visible Light Communication: Technology, Applications and Challenges A Survey*, International Journal of Advances in Engineering and Technology, Aug. 2015.
- [11] K. Cui, et al., *Line-of-sight Visible Light Communication System Design and Demonstration*, Communication Systems Networks and Digital Signal Processing (CSNDSP), 2010
- [12] J. Barry and J. Kahn, *Link design for non-directed wireless infrared communications*, Appl. Optics, vol. 34, no.19, pp. 37643776, July 1995
- [13] I. Lee, M. Sim and F. Kung, *Performance Enhancement of Outdoor Visible-Light Communication System using Selective Combining Receiver*, IET Optoelectronics, Vol. 3, 2009
- [14] J. W. Spencer, *Fourier Series Representation of the Sun*, Search, Vol. 2, p.172, 1971
- [15] NASA AMES, *Mars Climate Modeling Center*, Available from: <http://spacescience.arc.nasa.gov/mars-climate-modeling-group/brief.html>
- [16] D. Karunatilaka, et al., *LED Based Indoor Visible Light Communications: State of the Art*, IEEE Communication Surveys and Tutorials, Vol. 17, No. 3, Third Quarter 2015
- [17] Hamamatsu, *Si PIN Photodiode*, S3204/S3584 Series